Analysis of moisture risk in internally insulated masonry walls

Building and Environment 212 (2022) 108734

Contents lists available at ScienceDirect

Building and Environment

journal homepage: www.elsevier.com/locate/buildenv

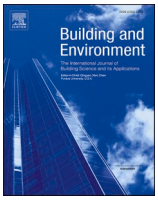

Analysis of moisture risk in internally insulated masonry walls

Xiaohai Zhou [a,*], Dominique Derome [b], Jan Carmeliet [a]

[a] Chair of Building Physics, ETH Zürich, Zürich, Switzerland
[b] Department of Civil and Building Engineering, Université de Sherbrooke, Sherbrooke, Canada

ARTICLE INFO

Keywords:
Internal insulation
ANN
Hygrothermal modeling
Masonry
WDR
Moisture risk

ABSTRACT

Due to the need to preserve the façades of valuable historical buildings, internal thermal insulation is often the only measure for energy retrofitting for such class of buildings. However, internal thermal insulation may lead to moisture damage risks. In this study, the influence of seven parameters, namely water absorption coefficient and diffusion resistance of the exterior render, wind-driven rain load, brick type, masonry structure, thermal insulation type and thermal conductance (U-value), of the internally retrofitted wall on moisture risk is analyzed. Two parameters, water absorption coefficient and wind-driven rain load, have a much larger influence on moisture risk. By comparison, brick type and masonry structure have a very small influence on moisture risk. The influence of U-value on moisture risk is dependent on the insulation system. An artificial neural network (ANN) model is trained based on hygrothermal simulation results. The results predicted by the ANN model are very close to the hygrothermal simulation results. The ANN model enables fast and reliable evaluation of moisture risks. Towards guidelines, the development of an index which would consider jointly render properties and wind-driven rain loads could support a more accurate evaluation of moisture risk in internally insulated masonry walls.

1. Introduction

Around 30% of buildings in Europe are historical buildings. In large part, these buildings are not well insulated and thus not energy efficient, which leads to high energy consumption of these buildings. For example, the average energy consumption of buildings built before 1920 in Switzerland is about 200 kWh/m^{2}a whereas it is below 100 kWh/m^{2}a for buildings after 2000 [1]. Therefore, the energy retrofit of historical buildings has great potential to reduce energy consumption and CO_2 emission in the building sector. Due to the need to preserve the façade of historical buildings, internal thermal insulation is often the only measure for energy retrofitting. It is possible to reduce the heating energy consumption in the historical buildings by 30–40% by retrofitting the existing walls with internal insulation [2]. However, internal thermal insulation is very risky due to the resulting lower temperature and consequently lower drying potential in the existing wall [3–10]. Moisture-related problems such as interstitial condensation and mould growth, freeze-thaw damage of the brickwork or decay in embedded wooden beams could then occur. An unthoughtfully planned retrofit with internal thermal insulation can lead to moisture-related problems in building envelopes and guidelines for such interventions are continuously improved.

Of interest here are load-bearing masonry buildings and, in particular, masonry finished with a render. As, wind-driven rain is the largest moisture source that influences the hygrothermal performance of building envelopes, exterior renders provide protection for masonry from moisture-related problems in regions with high wind-driven rain load [11]. Wall envelopes with hydrophobic or low capillary active renders show a much lower risk of moisture-related problems than those with capillary-active renders [6]. Water absorption coefficient (Acap) and vapour diffusion resistance (S_d) are the most important properties of renders determining their hygric behavior. The water absorption coefficient is a material property that characterizes the material's ability for wetting by liquid transport whereas the vapour diffusion resistance is a material property that describes the material's ability for drying by vapour diffusion. In Germany, the rain protection coefficient (C_{RP}) of renders, which is defined as the product of water absorption coefficient and vapour diffusion resistance (Acap* S_d), is required to be smaller than 0.2 kg/(mh$^{0.5}$) to avoid moisture-related problems in wall envelopes [12]. In addition, the water absorption coefficient should be smaller than 0.5 kg/(m^{2}h$^{0.5}$) and diffusion resistance smaller than 2.0 m. For wall envelopes with interior insulation, the C_{RP} requirement is stricter due to their lower drying potential. The rain protection coefficient is required to be smaller than 0.1 kg/(mh$^{0.5}$) according to the guidelines of

* Corresponding author.
E-mail address: xizhou@ethz.ch (X. Zhou).

https://doi.org/10.1016/j.buildenv.2021.108734
Received 3 October 2021; Received in revised form 20 December 2021; Accepted 26 December 2021
Available online 29 December 2021

the WTA (International Association for Science and Technology of Building Maintenance and Monuments Preservation) [13]. The most common internal thermal insulation systems are either vapour tight or capillary active. Vapour tight insulation systems limit vapour diffusion from the indoor environment to the cold surface of the original wall to avoid interstitial condensation. However, such insulation systems limit the drying to the indoor environment. By contrast, capillary active insulation systems are vapour open but can avoid interstitial condensation by redistributing moisture from the existing wall by capillary moisture transport towards the inside room allowing drying. However, moisture redistributed to the indoor environment may lead to higher indoor humidity level.

Many studies have been conducted to study the moisture risk of internally insulated masonry walls. For example, Vereecken and Roels compared the hygrothermal performance of a capillary active interior insulation system with a vapour tight system [9]. A better hygrothermal performance is observed for the capillary active interior insulation system. Morelli and Svendsen studied the effect of different WDR loads on moisture content in the internally insulated walls [3]. It is reported that WDR has a large influence on the moisture performance of the wooden beam embedded in internally insulated walls. Zhao et al. studied the performance of four capillary-active mineral insulation systems for interior retrofitting [14]. Compared to the vapour tight insulation system, all the four mineral insulation systems can reduce the moisture in the masonry wall by inward drying. Walker and Pavía presented that the vapour permeability of the interior insulation materials has a large influence on the moisture behaviour of the walls [15]. Vapour permeable insulation materials can lead to drying of wall envelope when RH in the environment is low. Hansen et al. presented that vapour open and capillary active interior insulation system performs better than vapour tight interior insulation system [16]. But the performance of the insulation system is strongly affected by the external hygrothermal loads. Finken et al. studied moisture risk of internally insulated walls with different insulation materials and thicknesses [17]. They reported that capillary active insulation needs to be combined with façade impregnation for regions with high precipitation. Jensen et al. reported that the diffusion-tight internal insulation systems perform better than the diffusion-open systems when exterior hydrophobisation is considered [18]. But the diffusion-open systems perform better when there is no hydrophobisation on the exterior surface. Guizzardi et al. studied the effect of exterior render type on moisture risk of wooden beams embedded in internally insulated masonry walls [4]. The exterior render strongly affects the risk of moisture related damage to embedded wooden structures in internally insulated masonry walls. Zhou et al. reported that the hygrothermal performance of interior insulated walls depends mainly on the moisture performance of the exterior finishing render [6]. For wall envelopes with relatively high capillary active renders, it is suggested to not use vapour barrier for retrofitting with interior insulation. For wall envelopes with less capillary active renders, whether or not to use vapour barrier depends mainly on the risk of water leakage and vapour resistance factor of the exterior render.

A limitation common to the previous studies is that the interaction between all possible factors on moisture risk is not considered. The previous studies consider mostly the influence of one or two factors on the moisture risk of internal insulation. Even for building envelopes with the same exterior render, hygrothermal performance could be affected by WDR load, wall structure, type of thermal insulation and level of thermal conductance, i.e. U-value of the insulation layer. For example, the influence of the exterior render on the hygrothermal performance is also dependent on WDR load. A wall envelope with a highly capillary active render does not necessarily lead to high moisture risk when the WDR load is very low. The performance of the interior insulation system is not only affected by the exterior render and WDR load but also by the wall structure and U value of the insulation system. The quantitative relation between the different factors and their combined influence on moisture risk is still not clear. A systematic study is yet to be performed to obtain an insight into quantitative relations between these factors. Evaluating the moisture risk of internally insulated masonry walls is challenging due to the complicated interactions of the above-mentioned factors. Furthermore, it is very demanding to build a hygrothermal model, as many meteorological data and material properties of building materials are required. In practice, much of these data are hardly available. Based on a broad analysis of the relevance of different parameters on moisture risk, more attention can be paid to the determining factors.

It is essential to develop a fast, easy and accurate method that can capture the relation between input parameters and moisture risk of internally insulated masonry walls. Artificial neural networks (ANNs) are algorithms designed to identify underlying relationships in a set of data through the process of imitating the way the human brain works. ANNs have been widely applied in building science. For example, Taffese and Sistonen used ANN for the prediction of the deterioration risk of concrete façade elements [19]. Kalogirou et al. applied ANN to predict the heating load of a building based on the input of areas of windows, walls, partitions and floors, the type of windows, walls and ceilings, and the designed room temperature [20]. Mechaqrane trained ANN for the prediction of the indoor air temperature of residential buildings [21]. Gawin et al. interpolated the sorption hysteresis of building materials with ANN [22]. Tzuc et al. estimated hygrothermal behavior for a green façade with ANN [23]. Tijskens et al. compared three popular types of neural networks for predicting moisture content, temperature and relative humidity time series in a masonry wall [24]. However, there is no study using ANNs for moisture risk assessment of internally insulated wall envelopes, pointing for the need to study the feasibility of using ANNs for such risk evaluation. The most common moisture problem in internally insulated wall envelopes is mould. Both temperature and humidity conditions affect mould growth on building materials. Also the exposure time to high humidity level affects mould growth. Mould is a more suitable indicator for moisture problems than humidity level. Therefore, it is necessary to develop an ANN that describes the nonlinear relation between mould growth and internally insulated envelope properties.

The paper aims to evaluate the moisture risk of internally insulated masonry walls. The influence of the significant parameters on moisture risks for internally insulated masonry walls is analyzed with a hygrothermal model. Then an ANN model is trained based on the results of hygrothermal simulations. The relative importance of the different parameters is analyzed. Finally, the ANN model is used for moisture risk evaluation of different internal thermal insulation scenarios.

2. Methodology

2.1. Hygrothermal model

A hygrothermal model is needed for studying the coupled moisture and heat transport in the wall envelopes. The governing equations for the hygrothermal model are the same as those in HAMFEM [6,25], and are solved using the finite element solver COMSOL.

Conservation of moisture:

$$\frac{\partial w}{\partial p_c}\frac{\partial p_c}{\partial t} + \nabla \cdot (g_l + g_v) = 0 \tag{1}$$

with

liquid flux:

$$g_l = -K_l \cdot \nabla p_c \tag{2}$$

vapour flux:

$$g_v = -\delta_v \cdot \frac{p_v}{\rho_l \cdot R_v \cdot T} \cdot \nabla p_c - \delta_v \cdot \frac{p_v}{\rho_l \cdot R_v \cdot T^2}(\rho_l \cdot L_v) \cdot \nabla T \tag{3}$$

Conservation of heat:

$$\left(c_0 \cdot \rho_0 + c_l \cdot w\right) \cdot \frac{\partial T}{\partial t} + \nabla \cdot \left(c_l \cdot \left(\mathrm{T} - \mathrm{T}_{ref}\right) \cdot g_l + \left(c_v \cdot \left(\mathrm{T} - \mathrm{T}_{ref}\right) + L_v\right) \cdot g_v = -\nabla\left(\lambda\left(w\right)\nabla T\right)\right) \tag{4}$$

where w is the moisture content (kg/m^3), p_c is the capillary pressure (Pa), g_l and g_v are the liquid and vapour flow (kg/m^{2}s), K_l is the liquid permeability (s), δ_v is the water vapour diffusion coefficient (s), p_v is the vapour pressure (Pa), ρ_l is the density of water (kg/m^3), R_v is the gas constant of water (J/kg K), T is the temperature (K), c_0 is the specific heat capacity of solids (J/kg K), c_l is the specific heat capacity of water (J/kg K), c_v is the specific heat capacity of vapour (J/kg K), ρ_0 is the density of solids (kg/m^3), T_{ref} is the reference temperature (273.15 K), L_v is the latent heat of vapourization (J/kg), $\lambda(w)$ is the thermal conductivity (W/mK), depending on moisture content. The coupled heat and mass transfer model was validated with HAMSTAD benchmark 4 and 5 [26].

2.2. Wall envelope

To consider the influence of wall structure, two types of wall structure are considered. The first wall structure has two wythes of brick and the second one has three wythes of brick (Fig. 1a and b). The thickness of the first wall structure is 285 mm whereas the thickness of the second wall structure is 415 mm. The cross-section of the wall envelopes shown between the dark blue dashed lines in Fig. 1a and b is considered in the 1 D simulations. Both wall structures consist of exterior render, brick, mortar and interior plaster. The material properties of the building materials are given in Appendix.

To study the influence of different renders, renders with different water absorption coefficients and vapour resistance factors are considered. The moisture transport properties of renders are obtained by changing those of a reference render. The chosen reference render is a mineral plaster from the WUFI database [27], which has a water absorption coefficient 0.1 kg/m^{2}h$^{0.5}$. The moisture transport properties of the other renders are the same as this reference render except for the liquid permeability and vapour resistance factor. The selected water absorption coefficient for the renders are 0.1, 0.2, 0.4, 0.6, 0.8 and 1.0 kg/m^{2}h$^{0.5}$, respectively. The selected water resistance factor for the renders are 5, 10, 20, 30, 40, 50 and 60, which corresponds to vapour diffusion resistance (Sd) of 0.1, 0.2, 0.4, 0.6, 0.8, 1.0 and 1.2 m. In total, 42 types of render with a combination of six water absorption coefficients and the seven vapour diffusion resistances are chosen. Liquid permeability is calculated as the product of moisture capacity and liquid diffusivity. The relation between liquid diffusivity D and water absorption coefficient A_{cap} is based on [28]:

$$D(w) = 3.8 \cdot \left(\frac{A_{cap}}{w_{cap}}\right)^2 \cdot 1000^{\frac{w}{w_{cap}}-1} \tag{5}$$

where $D(w)$ is the liquid diffusivity (m^2/s) and w_{cap} is the capillary moisture content (kg/m^3). The liquid permeability of the different renders is shown in Fig. 1c.

To consider the influence of different bricks, two bricks with very different material properties are considered. The liquid permeability of brick 1 is much larger than that of brick 2. In addition, brick 1 is much more vapour open than brick 2. The vapour resistance factor of brick 1 is 7.5 while it is 30.0 for brick 2. The material properties of the bricks are given in Appendix.

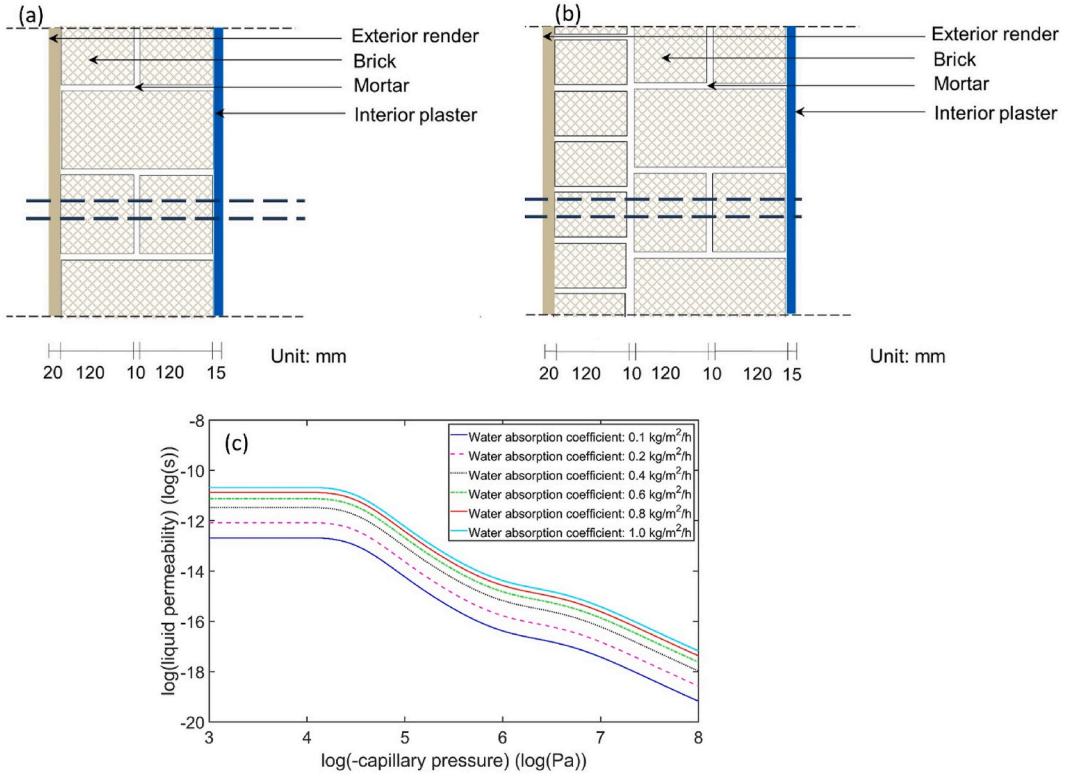

Fig. 1. (a) Geometry of wall envelope with two wythes of brick; (b) geometry of wall envelope with three wythes of brick; (c) liquid permeability of the renders with different water absorption coefficients.

2.3. Internal insulation systems

Two insulation systems for internal insulation are selected. The first system is a vapour tight system with glass wool and smart vapour retarder. The second one is a vapour open, capillary active system with calcium silicate. Glue mortar is needed to attach calcium silicate to the existing wall envelope. For the two insulation systems, a new interior plaster of 1.5 cm is added inwards of the insulation material. For the wall structure with two wythes of brick, the wall envelope is internally insulated to the following three U-values: 0.25, 0.35 and 0.45 W/m^{2}K. The thickness of the insulation materials is shown in Table 1. To ensure the same effect of insulation layer on hygrothermal performance, the insulation thickness used in either wall structure, two and three wythes of brick, is the same. The material properties of calcium silicate are from Ref. [29] and those of the glue mortar are from Ref. [9]. The material properties of glass wool and smart vapour retarder are from the WUFI database [27]. The details of the material properties are given in Appendix (see Table 3).

2.4. Initial and boundary conditions

Twelve years of meteorological data from October 1st 2005 to September 30th 2017 from the Meteoswiss station Zurich Kloten are used to drive the numerical model. The meteorological data include hourly outdoor air temperature, relative humidity, wind speed and wind direction at 10 m, solar radiation and horizontal rain. The initial conditions of the building envelope are a uniform temperature of 20 °C and a relative humidity of 60% RH. The first 2-year meteorological data is used to initialize the numerical model so that the simulated hygrothermal condition in the wall envelope is independent of the initial conditions. The remaining 10-year data is used for the analysis of the hygrothermal performance of wall envelopes.

The exterior convective heat transfer coefficient is calculated according to European standard EN15026 [30]. The exterior mass transfer coefficient (β_e) is related to the exterior convective heat transfer (h_e) by use of the Lewis analogy $\beta_e = h_e \times 7.7 \times 10^{-9}$, which assumes similarity between thermal and vapour boundary layers [31]. The wall orientation with the largest wind-driven rain load is selected for analysis, which is 240° from north (SSW). The wind-driven rain (WDR) load for wall envelope is calculated according to ASHRAE Standard 160 - Criteria for Moisture Control Design Analysis in Buildings [32], where the WDR intensity (R_{WDR}) is defined by the following equation:

$$R_{WDR} = R_h \times F_E \times F_D \times 0.2 \times V_{10} \times \cos\theta \tag{6}$$

where R_h is the horizontal rainfall amount (kg m^{-2}h^{-1} or mm h^{-1}); F_E is the rain exposure factor;F_D is the rain deposition factor; V_{10} is the wind speed at 10 m above ground (ms^{-1}); θ is the angle between the wind direction and the normal to the façade (rad). Factor F_E depends on the surrounding terrain and the height of the building, while Factor F_D describes the influence of the building itself. In the study, a rain exposure factor of 1.0 is selected. Five deposition factors of 0.0, 0.25, 0.5, 1.0 and 2.0 are selected to cover a different range of WDR load. Wind-driven rain load is calculated when the air temperature is above 0.0 °C. When the air temperature is at or below 0.0 °C, the precipitation is in the form of snow and no wind-driven rain load is considered deposited on the building envelope. The interior conditions are calculated according to the European standard EN15026 [30], in which indoor air temperature and relative humidity depend linearly on the outdoor temperature.

In total, 5040 simulations are performed. The simulations are run on a computer with an Intel(R) Core(TM) i7-9700K CPU @ 3.60 GHz, 128 GB of RAM and a 64 bit operating system. Eight simulations are run simultaneously. Each simulation takes around 80 minutes. For referencing, the following notation system is used to indicate the wall envelopes (e.g. CS-W2-B1-A0.2-SD0.2-U0.35-FD0.5): the first two letters represent the insulation system (CS: calcium silicate insulation system; GW: glass wool insulation system), the second label represents wall structure (W2: wall structure with 2 wythes of brick; W3: wall structure with 3 wythes of brick); the third brick type (B1: brick type 1; B2: brick type 2); the fourth water absorption of the exterior render (A0.2: the water absorption coefficient is 0.2 kg/m^{2}h$^{0.5}$); the fifth diffusion resistance of the exterior render (SD0.2: the diffusion resistance is 0.2 m); the sixth the U value of the wall envelope (U0.35: the U value of the internally insulated wall is 0.35 W/m^{2}K)); the seventh the rain deposition factor (FD0.5: the rain deposition factor is 0.5.).

Table 1
Insulation layer thickness for the different U values.

U-value (W/m^{2}K)	Insulation thickness (cm)	
	glass wool	calcium silicate
0.25	11.2	19.7
0.35	7.3	12.8
0.45	5.1	9.0

2.5. Moisture risk index

The moisture risk in the wall envelopes is evaluated with the VTT Mould Index [33–35]. The mould index is related to the mould growth conditions listed in Table 2 and ranges between 0 and 6.

The VTT model for mould growth in wood is described as follows [33]:

$$\frac{dM}{dt} = \frac{1}{7\cdot\exp(-0.68\ln T - 13.9\ln RH + 0.14W - 0.33SQ + 66.02)} k_1 k_2 \tag{7}$$

where M is the mould index level, T is the temperature, RH is the relative humidity, W is the timber species ($W = 0$ for pine and $W = 1$ for spruce), SQ is the surface quality ($SQ = 0$ for sawn surface, $SQ = 1$ for kiln-dried quality), factor k1 indicates the intensity of growth, factor k2 represents the moderation of the growth intensity when the mould index level (M) approaches the maximum peak value in the range of $4 < M < 6$.

$$k_1 = \begin{cases} 1 & when\ M \le 1 \\ \dfrac{2}{t_{M=3}/t_{M=1} - 1} & when\ M > 1 \end{cases} \tag{8}$$

The factor $t_{M=1}$ is time required for mould index level M to reach 1 and the factor $t_{M=3}$ is time required for mould index level M to reach 3. The parameter k2 is described as:

$$k_2 = \max[1 - \exp[2.3\cdot(M - M_{max})], 0] \tag{9}$$

where M_{max} is the largest possible value of the mould index, described as:

$$M_{max} = 1 + 7\cdot\frac{RH_{crit} - RH}{RH_{crit} - 100} - 2\cdot\left(\frac{RH_{crit} - RH}{RH_{crit} - 100}\right)^2 \tag{10}$$

where RH_{crit} is the limit relative humidity level for mould growth.

When the conditions are unfavorable for mould fungi to grow, ac-

Table 2
Mould index classification.

Index	Description of the growth rate
0	No growth
1	Small amounts of mould on surface (microscope), initial stages of local growth
2	Several local mould growth colonies on surface (microscope)
3	Visual findings of mould on surface, <10% coverage, or <50% coverage of mould (microscope)
4	Visual findings of mould on surface, 10–50% coverage, or, >50% coverage of mould (microscope)
5	Plenty of growth on surface, > 50% coverage (visual)
6	Heavy and tight growth, coverage about 100%

tivity of mould fungi will be deactivated and mould growth will decline. The decline of mould index is described with the following equation [33]:

$$\frac{dM}{dt} = \begin{cases} -0.00133, & when \quad t - t_1 \le 6h \\ 0, & when \quad 6h < t - t_1 \le 24h \\ -0.000667, & when \quad t - t_1 > 24h \end{cases} \tag{11}$$

where t_1 is the beginning time of the dry period.

The VTT model has also been expanded for other building materials other than wood [34,35]. For other building materials, the mould growth factors are calculated based on reference to pine:

$$k_1 = \begin{cases} \frac{t_{M=1,pine}}{t_{M=1}}, & when \ M < 1 \\ \frac{2\left(t_{M=3,pine} - t_{M=1,pine}\right)}{t_{M=3} - t_{M=1}}, & when \ M \ge 1 \end{cases} \tag{12}$$

where $t_{M=1,pine}$ and $t_{M=3,pine}$ refer to the values with the reference material pine.

The maximum mould index M_{max} which affects k_2 is calculated according to:

$$M_{max} = A + B \cdot \frac{RH_{crit} - RH}{RH_{crit} - 100} - C \cdot \left(\frac{RH_{crit} - RH}{RH_{crit} - 100}\right)^2 \tag{13}$$

where A, B, C and RH_{crit} depends on sensitivity class of the building materials. For medium resistant materials such as glass wool and calcium silicate, the value of RH_{crit} is 85% and the values of A, B and C are 0, 5 and 1.5, respectively.

The decline of mould index in building materials other than wood is:

$$\left(\frac{dM}{dt}\right)_{mat} = C_{mat}\left(\frac{dM}{dt}\right)_{pine} \tag{14}$$

where C_{mat} is the relative coefficient for mould index decline. Here, a relatively low decline coefficient of 0.2 is used for both glass wool and calcium silicate.

A mould index of 1 is often regarded as the maximum tolerable value since, from that moment, the germination process is assumed to start [36]. The most critical location for internal thermal insulation is the interface between the insulation layer and the existing wall. The maximum mould index achieved at this critical location over the 10-year period is used to assess moisture risk in the building envelopes.

2.6. ANN model

An ANN is a mathematical model that can learn the complex relationship between input and output and make predictions for new inputs. A feed-forward neural network consists of an input layer, one or more hidden layers, and an output layer (Fig. 2). The neuron is the basic unit of neural network and each neuron has a weight, a bias and an activation function. The weight of a neuron represents the signal strength of that neuron. There are several neurons in each layer. Input is first fed to the input layer. Then the neuron performs a linear transformation on the input through weights and biases. The next layer uses the output of the previous layer as input and performs a non-linear transformation with an activation function. An activation function defines how the weighted sum of the input is converted to an output. Common activation functions are rectified linear activation function, logistic activation function and hyperbolic tangent activation function. During the training process, the ANN calculates outputs based on inputs and minimizes the difference between calculated outputs and the desired outputs by changing the weights and biases of neurons. Then the trained ANN model can accurately capture the relationship between input variables and output variables.

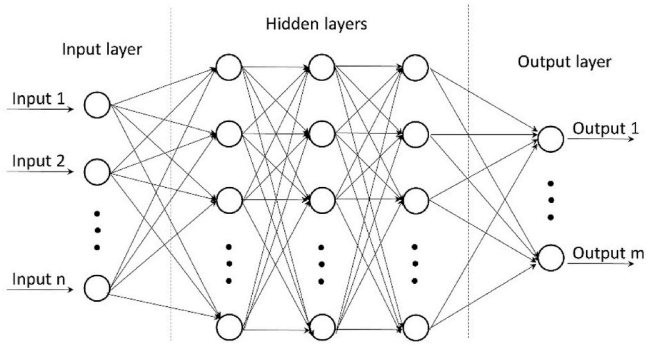

Fig. 2. Generic structure of an artificial neural network.

3. Results

3.1. Influence of the insulation system

Fig. 3 shows the maximum mould index in the wall envelopes with two wythes of brick 1 and the insulation material of calcium silicate and Fig. 4 shows the maximum mould index in the same wall envelopes but with glass wool as insulation material. The x-axis shows the different values of the water absorption coefficient, while the y-axis shows the vapour diffusion resistance. The blue lines are the contour lines for values of the maximum mould index from 1 to 3. The contour lines are obtained from linear interpolation of the maximum mould indexes. The columns show results for different U-values and the rows show results for different rain deposition factor F_D. Due to the medium resistant classification of calcium silicate and glass wool, the largest possible value of the mould index is 3.5, and the maximum mould index in these two figures is below 3.5. In general, wall envelopes with calcium silicate (Fig. 3) perform better than wall envelopes with glass wool (Fig. 4), and the maximum mould index is mostly smaller in the wall envelopes with calcium silicate. The contour lines of the maximum mould index are at a larger water absorption coefficient and diffusion resistance for the wall envelopes with calcium silicate. As an example, Fig. 5 shows relative humidity and mould index in two similar wall envelopes with different insulation system. The wall envelope CS-W2-B1-A0.6-SD0.6-U0.45-FD1.0 with calcium silicate shows a maximum mould index of 0.21, whereas it is 3.04 for the same wall envelope but with glass wool as insulation system. The large difference in the maximum mould index is due to the difference in relative humidity values. The calcium silicate insulation system can reduce relative humidity levels by redistributing moisture from the existing wall towards the indoor environment by capillary moisture transport. By comparison, the glass wool insulation system limits drying towards the indoor environment, resulting in a larger moisture level in the existing wall. In contrast, the humidity in the wall envelopes with the calcium silicate insulation system stays at a lower level.

3.2. Influence of water absorption coefficient and diffusion resistance

In general, the water absorption coefficient of the render has a very large influence on the maximum mould index (Figs. 3 and 4). An increase in the water absorption coefficient leads to a large increase in the maximum mould index. Similarly, an increase in vapour diffusion resistance of the render leads to a higher moisture risk and thus a larger mould index (Figs. 3 and 4). Compared to the water absorption coefficient, the effect of diffusion resistance on the maximum mould index is much smaller. The shape of the contour lines indicates that the change of maximum mould index is mainly along the x axis (Figs. 3 and 4). When the diffusion resistance is above a certain value, the contour lines become to some extent parallel to the y axis, which indicates that the influence of diffusion resistance on mould index becomes very small. We

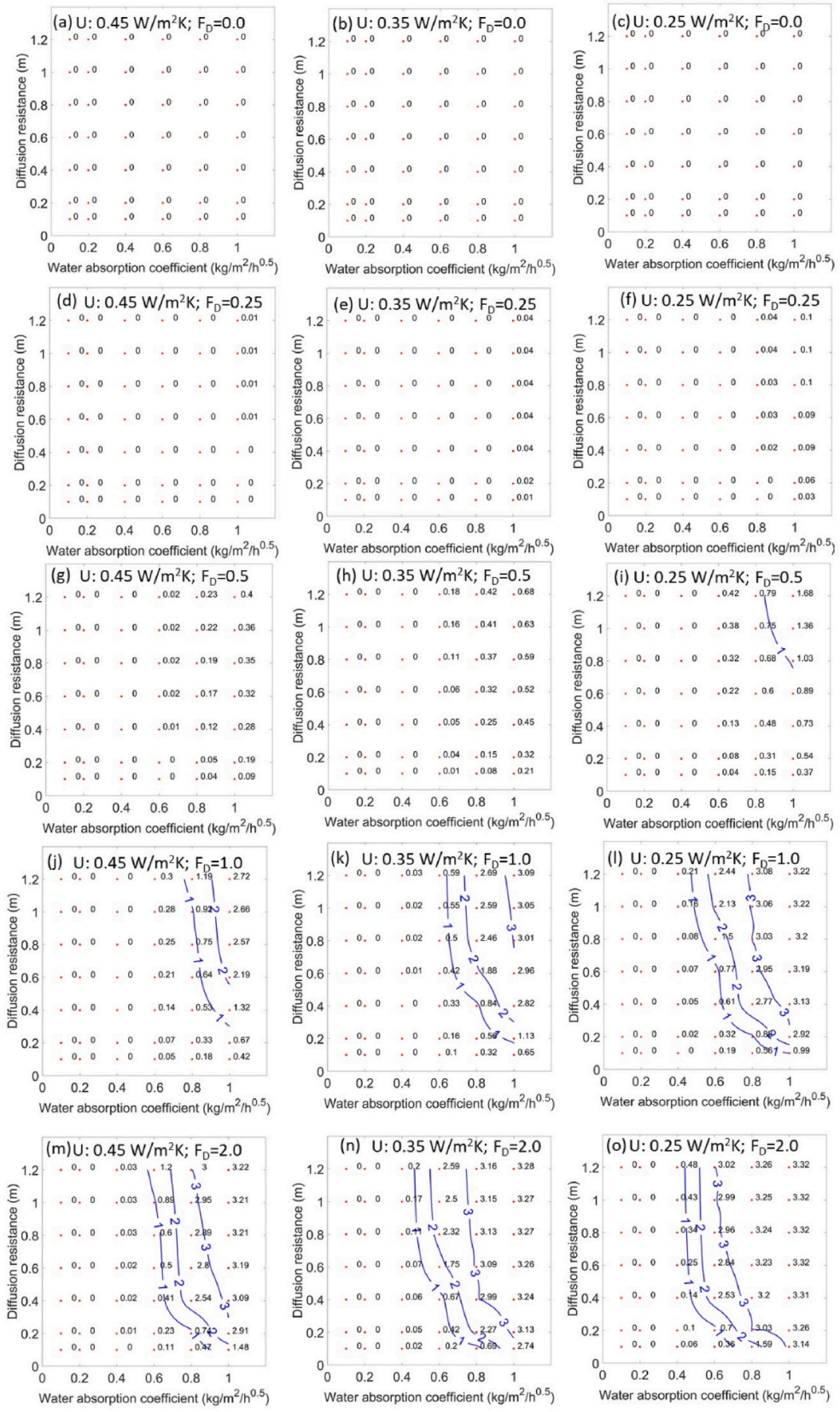

Fig. 3. Maximum mould index in wall envelopes with calcium silicate insulation in terms of diffusion resistance and water absorption coefficient (the blue lines are the contour lines) for different U-values (columns) and rain deposition factor F_D (rows). (For interpretation of the references to colour in this figure legend, the reader is referred to the Web version of this article.)

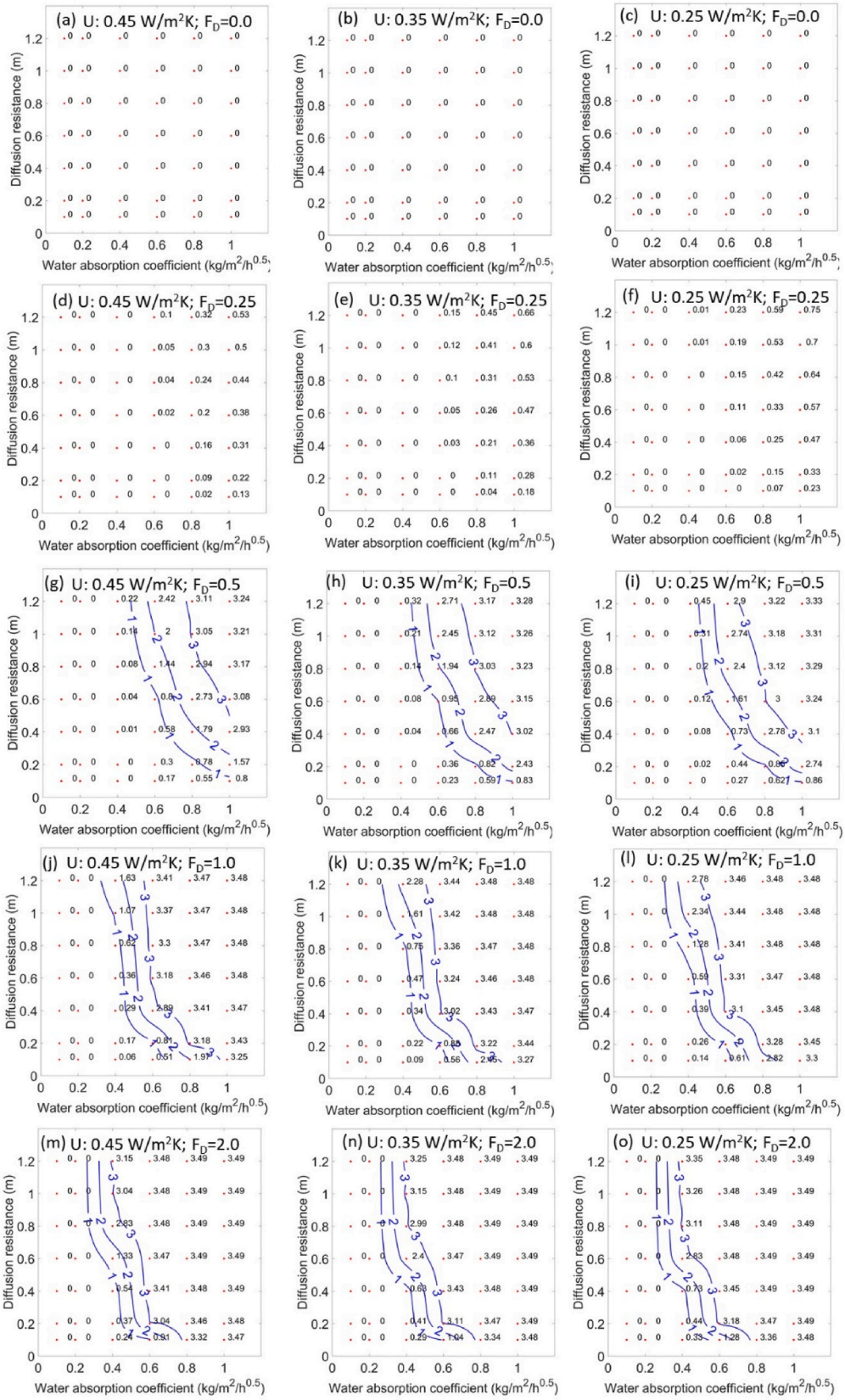

Fig. 4. Maximum mould index for wall envelopes with glass wool insulation in terms of diffusion resistance and water absorption coefficient (the blue lines are the contour lines) for different U-values (columns) and rain deposition factor F_D (rows). (For interpretation of the references to colour in this figure legend, the reader is referred to the Web version of this article.)

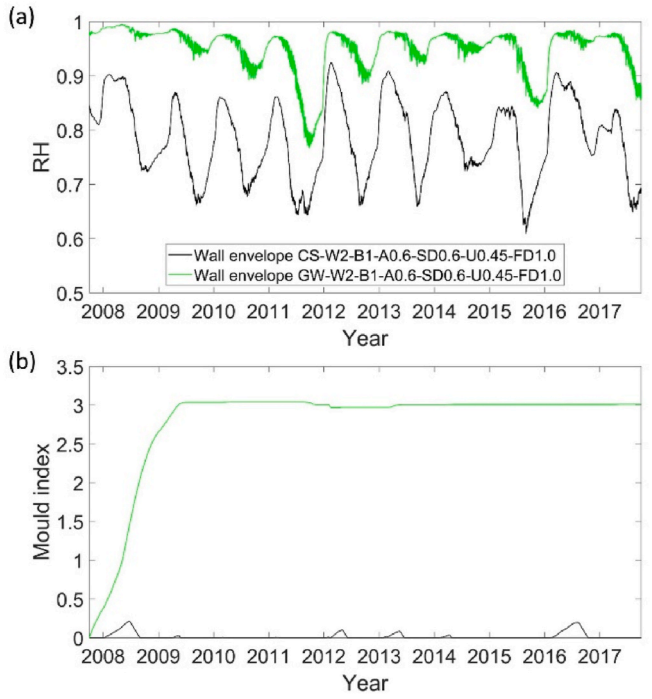

Fig. 5. (a) Relative humidity and (b) mould index in one instance of pair of wall envelopes with different insulation systems (black: calcium silicate; green: glass wool). (For interpretation of the references to colour in this figure legend, the reader is referred to the Web version of this article.)

found that the effect of the water absorption coefficient on the maximum mould index is strongly coupled with the rain deposition factor. Both water absorption coefficient and rain deposition factor are related to wetting by liquid transport, whereas vapour diffusion resistance is related to drying by vapour diffusion. The influence of water absorption coefficient and vapour diffusion resistance on the maximum mould index can be seen from the change of the maximum mould index along x-axis and y-axis. Generally speaking, in the region with the maximum mould index larger than 0 and smaller than 3, both water absorption coefficient and diffusion resistance can have an influence on the maximum mould index. An increase in the water absorption coefficient will lead to more absorption of water during rain events and thus to higher moisture risk. A decrease in the diffusion resistance will increase the drying capability and result in a considerable decrease in moisture risk. In the region with the maximum mould index larger than 3, the influence of both water absorption coefficient and diffusion resistance on the maximum mould index becomes small. The reason for this is that the wetting moisture source is much larger than the drying capability. A change in the water absorption coefficient or diffusion resistance does not alter the balance between wetting moisture source and drying capability.

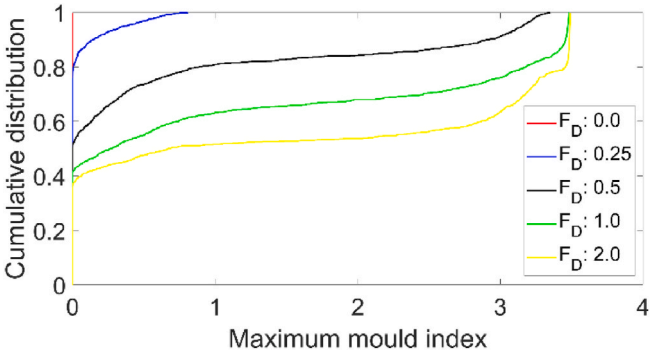

Fig. 6. Cumulative distribution curves of the maximum mould index for wall envelopes with different rain deposition factor F_D.

3.3. Influence of wind-driven rain load

In general, the WDR load has a very large influence on the mould index (Figs. 3 and 4). An increase in the rain deposition factor F_d leads to an increase in the mould index. Cumulative distribution curves show large differences in maximum mould index for different F_D values (Fig. 6). When the F_D value is 0.5, about 20% of the scenarios show a maximum mould index above 1.0. By comparison, about 40% of the scenarios show a maximum mould index above 1.0 when the F_D value is 1.0. The influence of wind-driven rain load on the mould index depends also on the properties of render. When the render has a low water absorption coefficient, the influence of wind-driven rain load on relative humidity and thus on moisture risk is small (Fig. 7a and b). The relative humidity is quite similar in the different envelopes even though they have different insulation systems and wind-driven rain loads. However, when the water absorption coefficient is relatively large, the wind-driven rain load has a very large influence on relative humidity and thus on mould index (Fig. 7c and d). In conclusion, water absorption coefficient and wind-driven rain are highly coupled parameters determining the maximum mould index.

3.4. Influence of U value

Generally, a smaller U value (higher insulation level) will lead to a larger maximum mould index (Figs. 3 and 4). This is because a smaller U value will lead to lower temperature in the masonry wall and thus lower drying potential. However, the influence of U value is strongly influenced by the type of insulation system. For the wall envelopes with a glass wool insulation system, the change of maximum mould index is not very sensitive to the change of U value. A decrease in the U value only leads to a small increase of the maximum mould index (Fig. 8b). By comparison, a decrease in the U value can lead to a much larger increase of the maximum mould index when the insulation system is calcium silicate (Fig. 8a). This difference is because the calcium silicate insulation system can transport moisture back to the inside environment by capillary transport. A smaller U value indicates larger insulation thickness and thus larger resistance for moisture flow. Consequently, the influence of U value is larger for the internal insulation system with calcium silicate.

3.5. Influence of brick type

Although the hygrothermal properties of the two brick types are very different, the difference in maximum mould index between the wall envelopes with bricks type 1 and 2 is in most cases limited (Fig. 9). For wall envelopes with calcium silicate and 2 wythes of masonry, only 17 out of 630 scenarios show a difference in maximum mould index larger than 0.3. Similarly, for wall envelopes with calcium silicate and 3 wythes of masonry, 24 out of 630 scenarios show a difference in maximum mould index larger than 0.3. By comparison, the difference in maximum mould index due to brick type is slightly larger for wall envelopes with glass wool than for walls with calcium silicate. 26 and 29 scenarios show a difference in maximum mould index larger than 0.3 for wall envelopes with 2 wythes of masonry and 3 wythes of masonry, respectively. The difference in moisture retention properties, liquid permeability and vapour resistance factor between brick 1 and 2 lead to the difference in RH and thus mould index in the different envelopes (Fig. 9). For wall envelopes with the insulation system of glass wool, wall envelopes with brick 2 show a larger relative humidity and thus larger mould index than brick 1 (Fig. 9c and d). Vapour retarder is used for the wall envelopes with glass wool insulation system and the drying can almost only occur towards the outside environment. Brick 1 has a much smaller vapour resistance factor than brick 2, which means a much

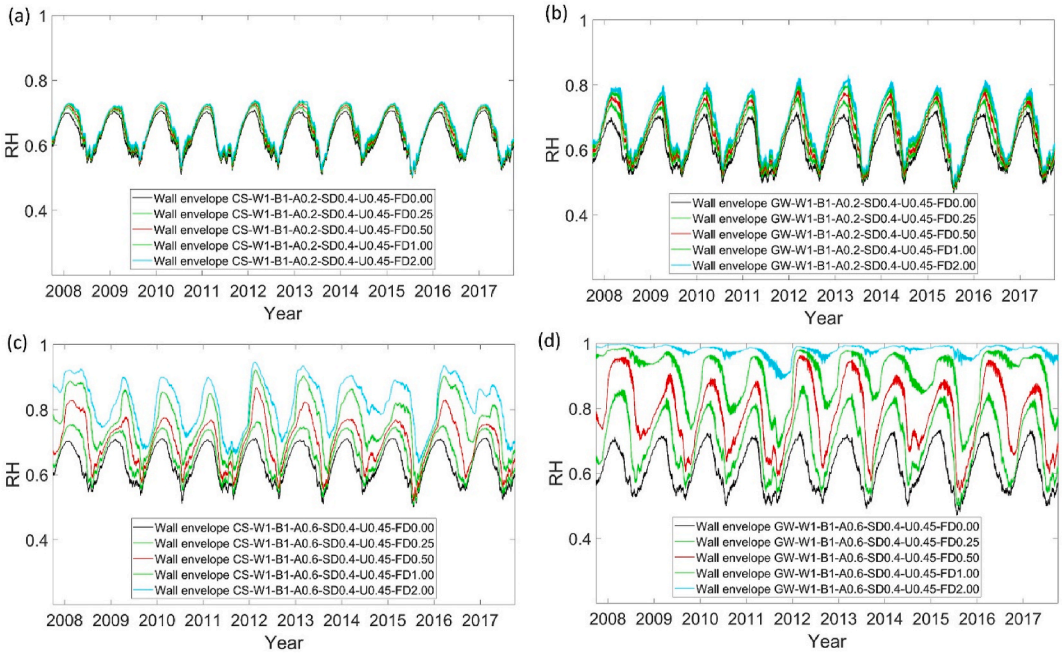

Fig. 7. Relative humidity for wall envelopes with low capillary absorption coefficient Acap and different rain deposition factor Fd with (a) calcium silicate and (b) glass wool insulation; relative humidity for wall envelopes with high capillary absorption coefficient Acap and different rain deposition factor Fd with (c) calcium silicate and (d) glass wool insulation.

larger drying capability of wall envelopes with brick 1. Thus, for wall envelopes with glass wool insulation system, the wall envelopes with brick 1 have generally lower RH and thus lower mould index than the wall envelopes with brick 2 (Fig. 10c and d). By comparison, for wall envelopes with calcium silicate insulation system, wall envelopes with brick 1 show larger relative humidity and mould index values than wall envelopes with brick 2 (Fig. 10a and b). When calcium silicate insulation system is used, the drying can not only occur towards the outside environment but also towards the inside environment. The drying capability is mostly larger towards inside than outside. Consequently, the influence of vapour resistance factor of brick on relative humidity is mostly very small. The influence of liquid permeability and moisture retention parameter is much larger. Brick 1 is more porous and can store more moisture content than brick 2. Also, brick 1 has larger liquid permeability than brick 2. Therefore, brick 2 with lower liquid permeability and lower moisture content shows a higher resistance against liquid water transport during the wetting period, which leads to faster drying during the drying period. Consequently, for wall envelopes with calcium silicate insulation system, the wall envelopes with brick 1 have generally larger RH and thus larger mould index than the wall envelopes with brick 2 (Fig. 9a and b).

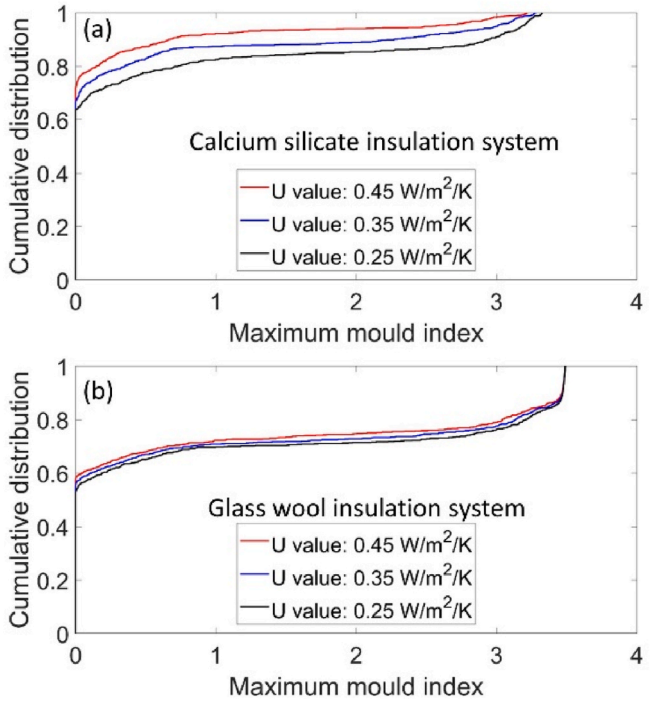

Fig. 8. (a) Influence of U value on the maximum mould index for wall envelopes with calcium silicate insulation system and (b) with glass wool insulation system.

3.6. *Influence of wall structure*

In general, the influence of wall structure on wall envelopes with a calcium silicate insulation system is small (Fig. 11). The maximum mould index difference between wall envelopes with 2 wythes of brick and 3 wythes of brick is small. The occurrence of drying toward the indoor environment makes the influence of the masonry wall structure small. By comparison, the wall structure has a much larger influence on wall envelopes with a glass wool insulation system, resulting in quite large differences in the mould index. It is clear that wall envelopes with 2 wythes of brick show larger maximum mould index than wall envelopes with 3 wythes of brick. Masonry walls with 2 wythes of brick have smaller moisture storage and smaller resistance to moisture flow than those with 3 wythes of brick. Consequently, masonry walls with 2 wythes of brick show larger moisture levels and thus higher maximum mould index.

3.7. *ANN analysis*

In order to consider the combined influence of different factors on

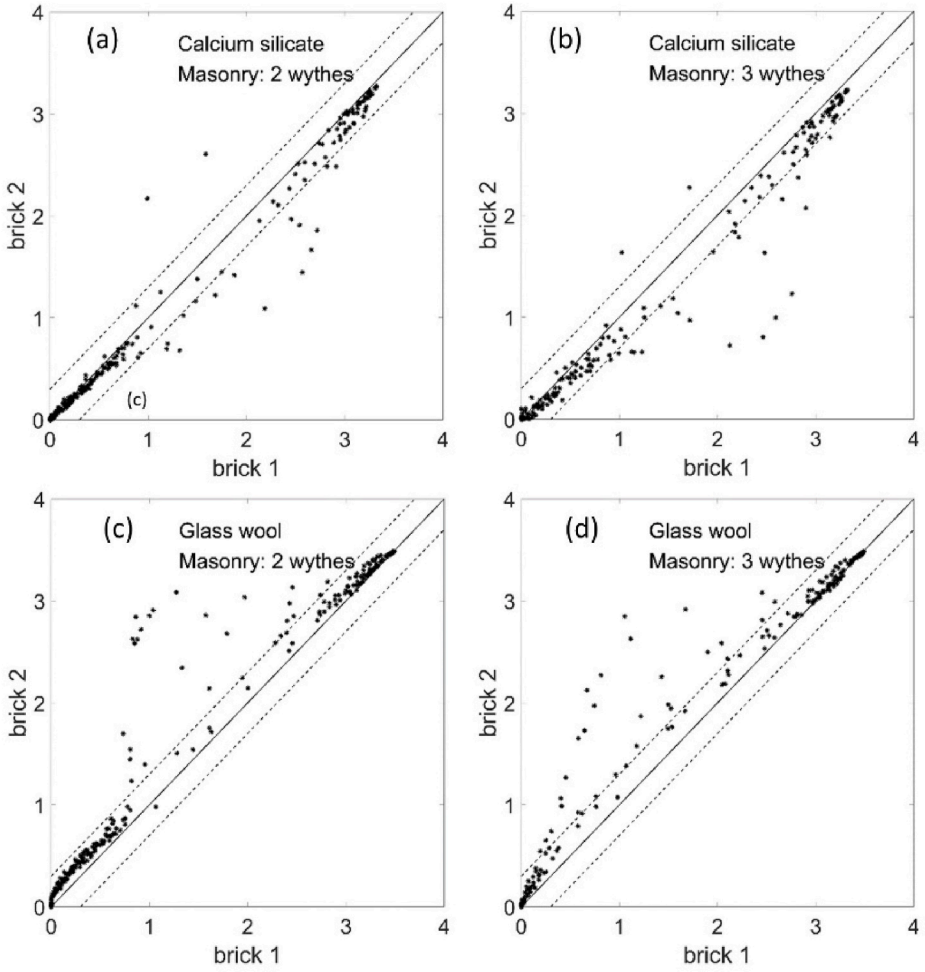

Fig. 9. Comparison of the maximum mould index in wall envelopes with bricks 1 and 2 for (a) insulation system: calcium silicate; masonry structure: 2 wythes of brick; (b) calcium silicate and 3 wythes of brick; (c) glass wool and 2 wythes of brick; (d) glass wool and 3 wythes of brick. (The dashed lines show ±0.3 mould index difference between brick 1 and 2.)

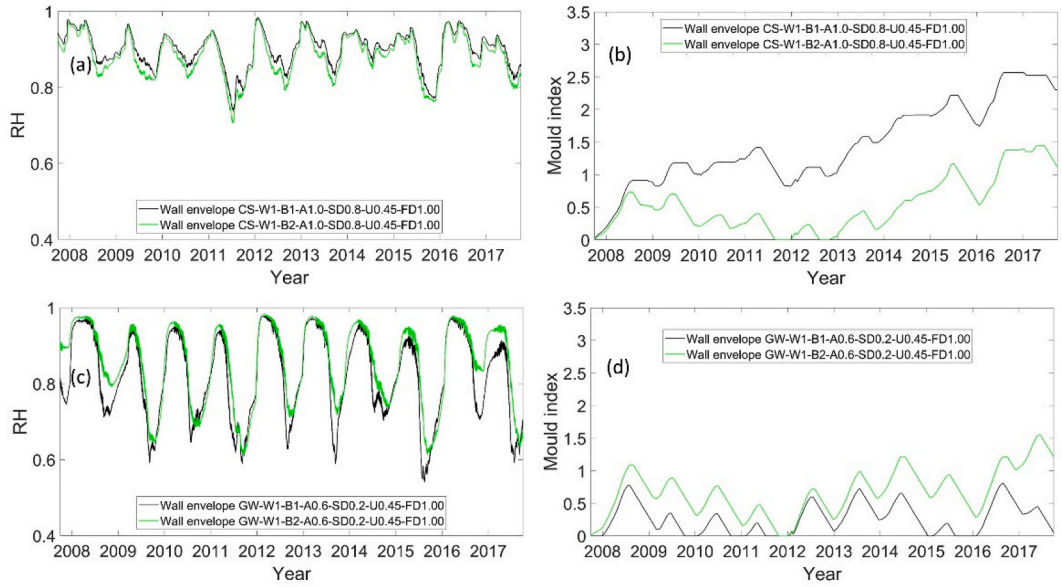

Fig. 10. (a) Relative humidity and (b) mould index in two wall envelops with calcium silicate insulation system; (c) Relative humidity and (d) mould index in two wall envelopes with glass wool insulation system (black: brick 1; green: brick 2). (For interpretation of the references to colour in this figure legend, the reader is referred to the Web version of this article.)

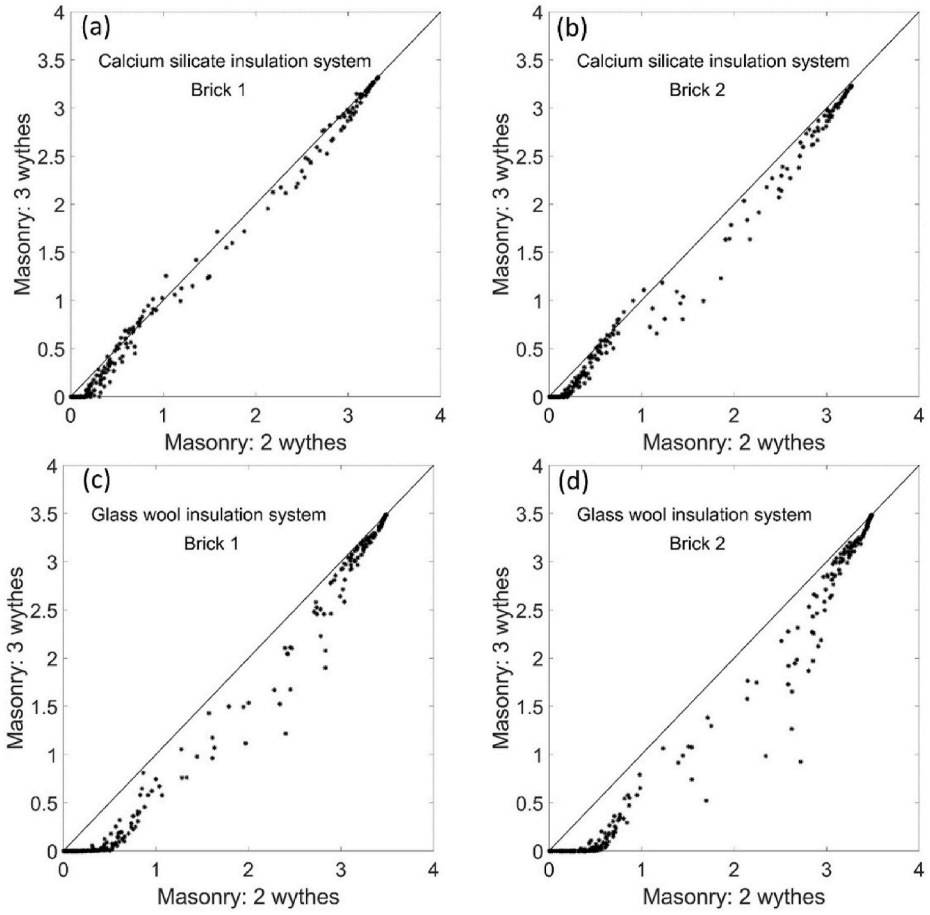

Fig. 11. Comparison of the maximum mould index in wall envelopes with 2 and 3 wythes of brick: (a) with calcium silicate insulation system and brick 1; (b) with calcium silicate insulation system and brick 2; (c) with glass wool insulation system and brick 1; (d) with glass wool insulation system and brick 2.

moisture risk, a global method is necessary to put into relations all inputs. ANN is an effective technique for capturing nonlinear behavior and predict the maximum mould index based on simple inputs. The 5040 hygrothermal simulation scenarios are used for the development of an ANN model. The Neural network toolbox in MATLAB is used for the ANN analysis. The type of artificial neural network used is feedforward neural network. Water absorption coefficient and diffusion resistance of the exterior render, rain deposition factor, U value of the internally insulated wall envelope, insulation type, brick type are the input variables and the maximum mould index is the output variable. The used activation function is the hyperbolic tangent sigmoid transfer function. The shares of samples used for training, validation and testing are 70%, 15% and 15%, respectively. The division of the data is performed randomly. The mean-squared error (MSE) of the simulated maximum mould index versus the ANN model predicated maximum mould index is used as the cost function. The Levenberg–Marquardt algorithm, also known as the damped least-squares method, is used as the optimization algorithm. The training samples are used to train the ANN model by fitting the parameters of the ANN model. The validation samples are used to fine tune the trained model and avoid overfitting problems. The test samples are used to test the performance of the trained model. The maximum number of epochs to train is set as 1000. The learning rate, which determines how much the weights can change following an observed error in the training set, is set as 0.5. Here we build an ANN model with 3 hidden layers. The number of neurons in each layer is 6, 10 and 6, respectively. Due to the small number of neurons, the training time is only around 5 s. The performance of the developed ANN model for predicting the maximum mould index is shown in Fig. 12a. The correlation coefficients (R) in training, validation and test are very close to 1.0, which indicates high accuracy of the trained ANN model.

The improved stepwise method [37] is used to quantify the input variable importance. The method eliminates one variable and quantifies its effect on the MSE of the ANN model. The variable that leads to larger MSE when eliminated is more important. Fig. 12b shows the importance of the different factors. Water absorption coefficient A_{cap} and rain deposition factor F_D have a much larger influence than the other factors. By comparison, the influence of brick type and wall structure is much smaller. The result is similar as that found in the analysis based on hygrothermal simulation.

The trained ANN model is very effective for predicting moisture risk. No hygrothermal simulation is needed to evaluate the moisture risk for this given climate. The only inputs are the values of the input factors. As an example, we consider a wall envelope with two wythes of brick 1, a measured water absorption coefficient and diffusion resistance of the exterior render of 0.5 kg/m^2/h and 0.6 m, a U value of the internally insulated wall of 0.25 W/m^2/K and we assume a rain deposition factor is 0.6. Contemplating a measurement uncertainty on water absorption coefficient, diffusion resistance and rain deposition factor is 30%, we evaluate the influence of these factors by changing their values by −30%, 0%, 30%. The time needed for the application of the trained ANN model for this prediction is less than 1 s. Fig. 13a presents that the ANN predicted results have very high correlation with the results obtained by hygrothermal simulations. Fig. 13b shows the maximum mould index at the different scenarios. For all the scenarios with calcium silicate, the maximum mould index is smaller than 1.0. By comparison, for all the scenarios with glass wool, as much as 41% of the scenarios have maximum mould index larger than 1.0, actually reaching 3.34. We conclude that, in this example, there is no moisture damage risk with

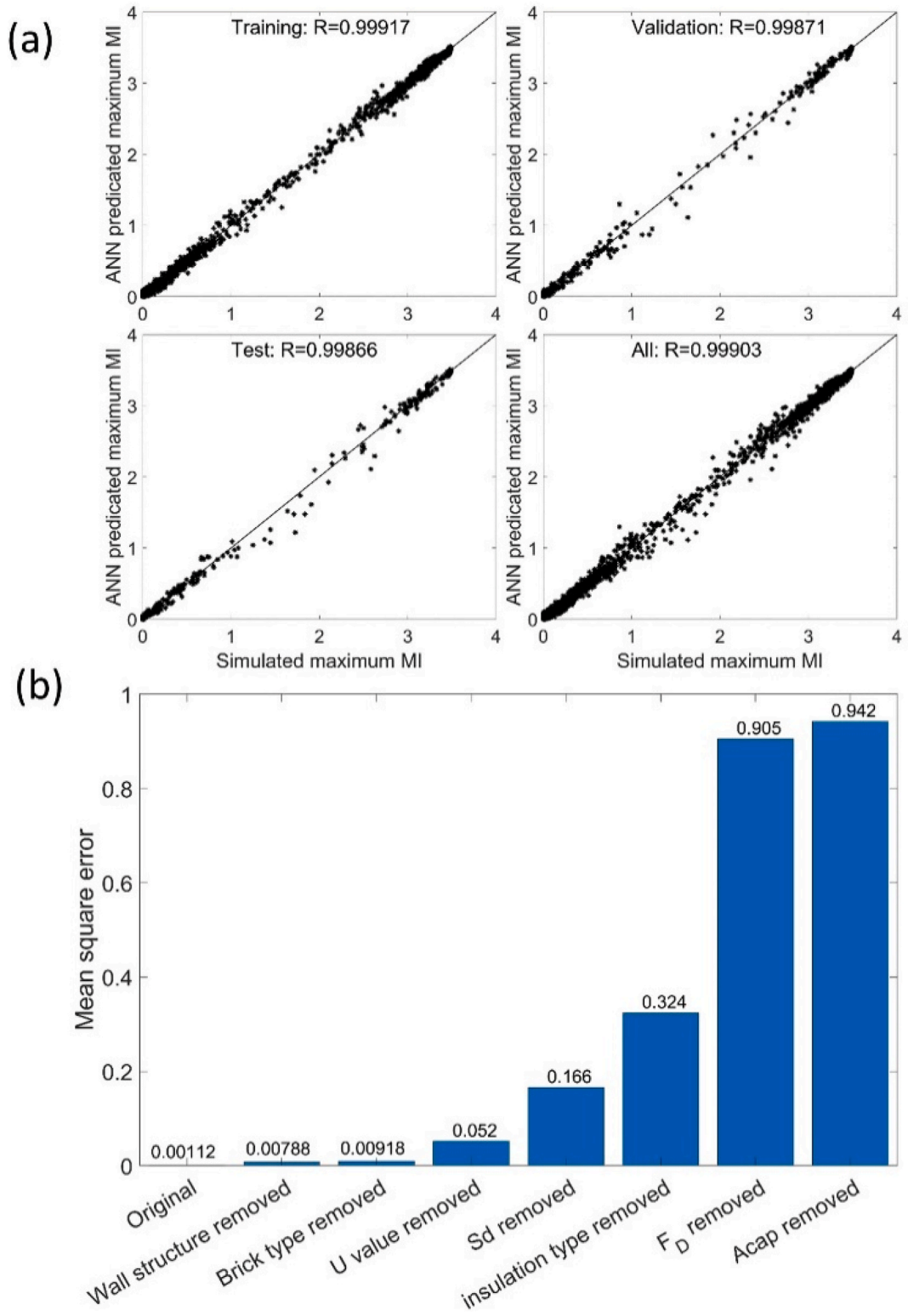

Fig. 12. (a) Regression plot for the maximum mould index from hygrothermal simulations vs. ANN predicted mould index in training, validation, test and total (MI: maximum mould index); (b) Importance of the different factors on the maximum mould index.

calcium silicate as internal thermal insulation even taking into account the uncertainties on input parameters. By comparison, the influence of the uncertainties on moisture risk for envelopes with glass wool insulation is very large. A reliable evaluation depends on the accurate determination/estimation of the most influential parameters such as the water absorption coefficient and the rain deposition factor.

4. Discussion

Overall, in this study, the wall envelopes with calcium silicate as inside thermal insulation perform much better than those with glass wool. However, glass wool is commonly preferred as interior wall insulation, as long as the wall envelope does not have risk of moisture-

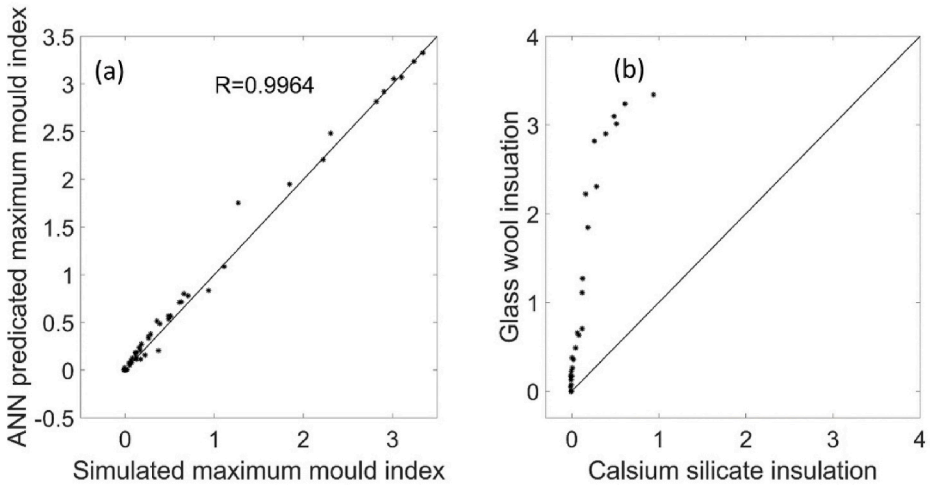

Fig. 13. (a) Comparison of the results by ANN and hygrothermal simulation; (b) Maximum mould index for the different uncertainty scenarios.

related problems. On the one hand, glass wool has a thermal conductivity much lower than calcium silicate, and for the same U-value, using glass wool as interior thermal insulation results in less space loss. On the other hand, calcium silicate insulation transports moisture back to the indoor environment and thus leads to a higher humidity level in the indoor environment, and sufficient ventilation is needed to lower the humidity level in the room. Nevertheless, calcium silicate should be used as interior wall insulation when the wall envelope presents a higher moisture risk due to climatic, topographic or other factors. For internal thermal insulation, it is favorable to replace the existing outside render with a new one, showing a much lower capillary absorption coefficient or even hydrophobic behavior, meanwhile being vapour open. In this case, the internally insulated wall envelope will not show moisture risk even exposed to a relatively high wind-driven rain load. A decrease of the U value of the retrofitted wall envelope will only increase moisture risk slightly.

The WTA guideline requires a rain protection coefficient smaller than 0.1 kg/(mh$^{0.5}$) to avoid moisture risk. Our study reaches a similar result. All the scenarios with a rain protection coefficient smaller than 0.1 kg/(mh$^{0.5}$) have a maximum mould index smaller than 1 (Fig. 14). However, many scenarios with rain protection coefficient larger than 0.1 kg/(mh$^{0.5}$) have also a maximum mould index smaller than 1. The WTA guideline only considers the influence of the exterior render and implicitly assumes that water absorption coefficient and diffusion resistance have the same influence on moisture risk. In this study, it is found that water absorption coefficient and WDR load are the two most important factors affecting moisture risk. They affect moisture risk much more than the diffusion resistance. Thus, it is necessary to develop a new index that considers not only the properties of the exterior render but also the WDR load, taking into account that a lower WDR load would allow a higher capillary absorption coefficient and vice versa.

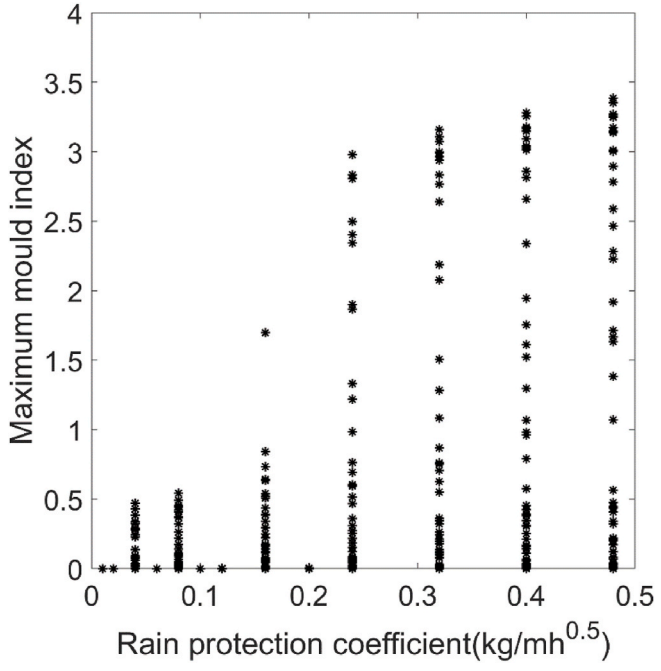

Fig. 14. Relation between rain protection coefficient and the maximum mould index for all simulated cases.

The trained ANN model is found to be very effective for a parametric analysis of moisture risk of internal thermal insulation projects. Prediction results can be obtained almost instantly with the ANN trained model. The aforementioned analysis demonstrates that water absorption coefficient and WDR load have a much larger influence than masonry structure and brick type. Water absorption coefficient and WDR load should be determined accurately. A small uncertainty of these parameters will have a relatively large influence on the evaluation of the moisture risk. The selection of U value and internal thermal insulation system can be evaluated with the application of the ANN model. Further work should provide a methodology for the selection of the parameters and for the extent of the range of values and the number of values to select for each parameter.

5. Conclusions

Hygrothermal simulations are performed to evaluate the influence of different parameters on moisture risk in wall envelopes after internal thermal retrofitting. The moisture risk is evaluated with the mould index. It is found that WDR load and the water absorption coefficient of the exterior render have the largest influence on moisture risk. By comparison, diffusion resistance of the exterior render, the U value of the retrofitted wall, masonry structure and brick properties have a much smaller influence. Wall envelopes with capillary active insulation system perform much better than those with vapour tight insulation system. The influence of U value on moisture risk is dependent on the insulation system. For wall envelopes with glass wool insulation, the U value has a very small influence on moisture risk. By comparison, the influence of the U value is much larger when calcium silicate system is used. An ANN model is trained based on the hygrothermal simulation results. The trained ANN model can accurately capture the nonlinear relationship between input variables and the maximum mould index. The predicted

results by the ANN model is very close to the results by hygrothermal simulation. The trained ANN model is very effective for predicting moisture risk. As rain protection coefficient considers only properties of render, there is a need to develop a new index which considers not only properties of render but also the effect of WDR load for accurate evaluation of moisture risk in internally insulated masonry walls.

CRediT authorship contribution statement

Xiaohai Zhou: Writing – review & editing, Writing – original draft, Validation, Software, Methodology, Conceptualization, Funding acquisition. **Dominique Derome:** Writing – review & editing, Supervision, Funding acquisition. **Jan Carmeliet:** Writing – review & editing, Supervision, Funding acquisition.

Declaration of competing interest

The authors declare that they have no known competing financial interests or personal relationships that could have appeared to influence the work reported in this paper.

Acknowledgement

This research project is part of the Swiss Competence Center for Energy Research SCCER FEEB&D of the Swiss Innovation Agency Innosuisse (CTI.1155002539). The meteorological data have been provided by MeteoSwiss, the Swiss Federal Office of Meteorology and Climatology. Derome acknowledges support from Canada Research Chair and NSERC Discovery programs.

Appendix

The capillary pressure curve of the building materials is described using a multimodal function of the van Genuchten model [38,39]:

$$w = w_{cap} \sum_{i=1}^{N} \frac{k_i}{(1 + abs(a_i \cdot p_c) n_i)^{m_i}} \tag{15}$$

where w_{cap} is the capillary saturation moisture content (kg/m3); p_c is the capillary pressure (Pa); k is the weighting parameter, a, m and n are fitting parameters where $m = 1\text{-}1/n$; N is the modal number and i is the counter.

The thermal conductivity of the building materials is given by:

$$\lambda = \lambda_{dry} + a \cdot w \tag{16}$$

where $\lambda_{dry}$is the dry thermal conductivity (W/mK), a is a parameter describing the influence of moisture content on thermal conductivity (Wm^2/kg K), w is the moisture content (kg/m^3).

The vapour diffusion coefficient of the building materials is given by:

$$\delta_v = \frac{26.1 \cdot 10^{-6}}{\mu_{dry} R_v T} \cdot \frac{1 - \frac{w}{w_{cap}}}{(1-p) \cdot \left(1 - \frac{w}{w_{cap}}\right)^2 + p} \tag{17}$$

where μ_{dry} is the vapour resistance factor, R_v is the gas constant of water (J/kg K), T is the temperature (K), w is the moisture content (kg/m^3), w_{cap} is the capillary saturated moisture content (kg/m^3), p is equal to 0.497.

The material properties of the building materials are given in Table 3 and Fig. 15.

Table 3
Material properties of the building materials

	Density (kg/m^3)	Heat capacity (J/kg/K)	Capillary moisture content (kg/m^3)	Moisture retention parameters				μ_{dry} (−)	Thermal conductivity		K_l (s)
				N	k	a	n		λ_{dry} (W/mK)	a	
Exterior render [27]	1900	850	210	3	0.21	5.00e-5	1.6	5–60	0.80	3.4e-3	Fig. 2
					0.36	2.60e-5	1.2				
					0.43	2.00e-7	1.4				
Brick 1 [26]	1600	1000	373.5	2	0.46	4.80e-5	1.5	7.5	0.68	0.0	Fig. 15a
					0.54	2.04e-5	3.8				
Brick 2 [26]	2005	840	150	2	0.30	1.25e-5	1.65	30	0.50	4.5e-3	Fig. 15a
					0.70	1.85e-5	6.0				
Mortar [26]	230	920	700	2	0.20	5.10e-5	1.5	50	0.60	5.6e-4	Fig. 15a
					0.80	4.1e-7	3.8				
Interior plaster [25]	79	790	812	2	0.85	2.7e-6	3.6	3	0.20	4.5e-3	Fig. 15a
					0.15	2.6e-6	1.7				
Calcium silicate [29]	270	1000	400	2	0.25	3.8e-5	1.7	5.6	0.06	5.6e-4	Fig. 15a
					0.75	1.3e-5	2.1				
Glue mortar [9]	1680	1000	213.4	2	0.48	3.5e-8	2.0	32	0.70	0.0	Fig. 15a
					0.52	1.6e-6	3.0				
Glass wool [27]	38	850	387	2	0.25	3.8e-5	1.7	1.3	See Fig. 15c		1e-30
					0.75	1.3e-5	2.1				
Smart vapour retarder [27]	83	1800	232	2	0.30	4.0e-5	1.9	See Fig. 15b	1.0	0.0	1e-30
					0.70	2.0e-5	2.0				

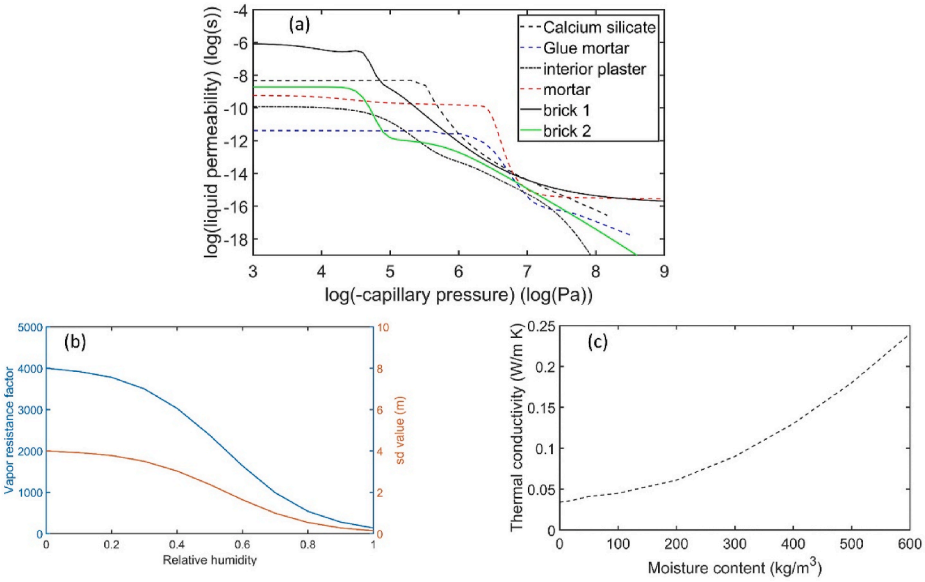

Fig. 15. (a) Liquid permeability of the building materials; (b) vapour resistance factor and sd value of the smart vapour retarder; (c) thermal conductivity of glass wool.

References

[1] Amt für Abfall, Wasser, Energie und Luft (AWEL), Energie in Wohnbauten 2018, Zürich, Switzerland, 2018.

[2] E.J. de Place Hansen, K.B. Wittchen, Energy savings due to internal façade insulation in historic buildings, in: 3rd Int. Conf. Energy Effic. Hist. Build. (EEHB2018), Visby, Sweden, Sept. 26th to 27th, 2018, Uppsala University, 2018, pp. 22–31.

[3] M. Morelli, S. Svendsen, Investigation of interior post-insulated masonry walls with wooden beam ends, J. Build. Phys. 36 (2013) 265–273.

[4] M. Guizzardi, J. Carmeliet, D. Derome, Risk analysis of biodeterioration of wooden beams embedded in internally insulated masonry walls, Construct. Build. Mater. 99 (2015) 159–168.

[5] M. Harrestrup, S. Svendsen, Internal insulation applied in heritage multi-storey buildings with wooden beams embedded in solid masonry brick façades, Build. Environ. 99 (2016).

[6] X. Zhou, J. Carmeliet, D. Derome, Influence of envelope properties on interior insulation solutions for masonry walls, Build. Environ. 135 (2018) 246–256.

[7] X. Zhou, D. Derome, J. Carmeliet, Hygrothermal modeling and evaluation of freeze-thaw damage risk of masonry walls retrofitted with internal insulation, Build. Environ. 125 (2017) 285–298.

[8] X. Zhou, J. Carmeliet, D. Derome, Assessment of moisture risk of wooden beam embedded in internally insulated masonry walls with 2D and 3D models, Build. Environ. 193 (2021) 1–16.

[9] E. Vereecken, S. Roels, Capillary active interior insulation: do the advantages really offset potential disadvantages? Mater. Struct. 48 (2015) 3009–3021.

[10] T. Odgaard, S.P. Bjarløv, C. Rode, Interior insulation–Experimental investigation of hygrothermal conditions and damage evaluation of solid masonry façades in a listed building, Build. Environ. 129 (2018) 1–14.

[11] H. Künzel, Criteria defining rain protecting external rendering systems, Energy Proc. 78 (2015) 2524–2529.

[12] D.E.I. 4108-3, Thermal Protection and Energy Economy in Buildings Part 3: Protection against Moisture Subject to Climate Conditions Requirements and Directions for Design and Construction, 2013.

[13] W.T.A. Merkblatt, 6-4-01, Innendämmung nach WTA I: Planungsleitfaden, Wissenschaftlich-Technische Arbeitsgemeinschaft Für Bauwerkserhaltung Und Denkmalpfl, EV, München, 2009.

[14] J. Zhao, J. Grunewald, U. Ruisinger, S. Feng, Evaluation of capillary-active mineral insulation systems for interior retrofit solution, Build. Environ. 115 (2017) 215–227.

[15] R. Walker, S. Pavía, Thermal and moisture monitoring of an internally insulated historic brick wall, Build. Environ. 133 (2018) 178–186.

[16] T.K. Hansen, S.P. Bjarløv, R.H. Peuhkuri, M. Harrestrup, Long term in situ measurements of hygrothermal conditions at critical points in four cases of internally insulated historic solid masonry walls, Energy Build. 172 (2018) 235–248.

[17] G.R. Finken, S.P. Bjarløv, R.H. Peuhkuri, Effect of façade impregnation on feasibility of capillary active thermal internal insulation for a historic dormitory–A hygrothermal simulation study, Construct. Build. Mater. 113 (2016) 202–214.

[18] N.F. Jensen, T.R. Odgaard, S.P. Bjarløv, B. Andersen, C. Rode, E.B. Møller, Hygrothermal assessment of diffusion open insulation systems for interior retrofitting of solid masonry walls, Build. Environ. (2020) 107011.

[19] W.Z. Taffese, E. Sistonen, Neural network based hygrothermal prediction for deterioration risk analysis of surface-protected concrete façade element, Construct. Build. Mater. 113 (2016) 34–48.

[20] S.A. Kalogirou, C. Neocleous, C.N. Schizas, Artificial neural networks used for estimation of building heating load, in: Proceedings of the International Conference CLIMA 2000, Brussels, Belgium, 1997.

[21] A. Mechaqrane, M. Zouak, A comparison of linear and neural network ARX models applied to a prediction of the indoor temperature of a building, Neural Comput. Appl. 13 (2004) 32–37.

[22] D. Gawin, M. Lefik, B.A. Schrefler, ANN approach to sorption hysteresis within a coupled hygro-thermo-mechanical FE analysis, Int. J. Numer. Methods Eng. 50 (2001) 299–323.

[23] O.M. Tzuc, O.R. Gamboa, R.A. Rosel, M.C. Poot, H. Edelman, M.J. Torres, A. Bassam, Modeling of hygrothermal behavior for green facade's concrete wall exposed to nordic climate using artificial intelligence and global sensitivity analysis, J. Build. Eng. 33 (2021) 101625.

[24] A. Tijskens, S. Roels, H. Janssen, Neural networks for metamodelling the hygrothermal behaviour of building components, Build. Environ. 162 (2019) 106282.

[25] H. Janssen, B. Blocken, J. Carmeliet, Conservative modelling of the moisture and heat transfer in building components under atmospheric excitation, Int. J. Heat Mass Tran. 50.

[26] C.-E. Hagentoft, A.S. Kalagasidis, B. Adl-Zarrabi, S. Roels, J. Carmeliet, H. Hens, J. Grunewald, M. Funk, R. Becker, D. Shamir, Assessment method of numerical prediction models for combined heat, air and moisture transfer in building components: benchmarks for one-dimensional cases, J. Therm. Envelope Build. Sci. 27 (2004) 327–352.

[27] H.M. Künzel, Simultaneous Heat and Moisture Transport in Building Components, One-And Two-Dimensional Calc. Using Simple Parameters, IRB-Verlag Stuttgart, 1995.

[28] H.M. Künzel, Effect of interior and exterior insulation on the hygrothermal behaviour of exposed walls, Mater. Struct. 31 (1998) 99–103.

[29] S. Roels, J. Carmeliet, H. Hens, O. Adan, H. Brocken, R. Cerny, Z. Pavlik, A.T. Ellis, C. Hall, K. Kumaran, A comparison of different techniques to quantify moisture content profiles in porous building materials, J. Therm. Envelope Build. Sci. 27 (2004) 261–276.

[30] EN 15026, Hygrothermal Performance of Building Components and Building Elements–Assessment of Moisture Transfer by Numerical Simulation, 2007.

[31] H.S.L. Hens, Building Physics-Heat, Air and Moisture: Fundamentals and Engineering Methods with Examples and Exercises, John Wiley & Sons, 2017.

[32] ASHRAE Standard 160,Criteria for Moisture Control Design Analysis in Buildings, ASHRAE, Atlanta, 2009.

[33] A. Hukka, H.A. Viitanen, A mathematical model of mould growth on wooden material, Wood Sci. Technol. 33 (1999) 475–485.

[34] T. Ojanen, H. Viitanen, R. Peuhkuri, K. Lähdesmäki, J. Vinha, K. Salminen, Mold growth modeling of building structures using sensitivity classes of materials, 11th Int. Conf. Therm. Perform. Exter. Envel. Whole Build. Build. XI (2010).

[35] T. Ojanen, R. Peuhkuri, H. Viitanen, K. Lähdesmäki, J. Vinha, K. Salminen, Classification of material sensitivity–new approach for mould growth modeling, in: 9th Nord, Symp. Build. Phys., 2011, pp. 867–874.

[36] E. Vereecken, S. Roels, Review of mould prediction models and their influence on mould risk evaluation, Build. Environ. 51 (2012) 296–310.

[37] M. Gevrey, I. Dimopoulos, S. Lek, Review and comparison of methods to study the contribution of variables in artificial neural network models, Ecol. Model. 160 (2003) 249–264.

[38] W. Durner, Predicting the unsaturated hydraulic conductivity using multi-porosity water retention curves, Indirect Methods Estim. Hydraul. Prop. Unsaturated Soils. (1992) 185–202.

[39] M.T. van Genuchten, A closed-form equation for predicting the hydraulic conductivity of unsaturated Soils1, Soil Sci. Soc. Am. J. 44 (1980) 892.